Published in final edited form as:
Comp Biochem Physiol A Mol Integr Physiol. 2007 May ; 147(1): 84–93.

Two distinct aquaporin-4 cDNAs isolated from medullary cone of quail kidney ☆

Yimu Yang[a], **Yujun Cui**[a], **Zheng Fan**[a], **George A. Cook**[b], and **Hiroko Nishimura**[a,*]

a *Department of Physiology, University of Tennessee Health Science Center, Memphis, TN 38163, USA*

b *Department of Pharmacology, University of Tennessee Health Science Center, Memphis, TN 38163, USA*

Abstract

Water deprivation or arginine vasotocin upregulates aquaporin-2 (AQP2) expression in apical and subapical regions of medullary collecting duct (CD) cells of *Coturnix coturnix* quail (q) kidneys. We therefore aimed to determine whether the CD has AQPs mediating water exit from the intracellular to the extracellular (interstitial) space. Using a homologue cloning technique, we isolated two distinct qAQP4 cDNAs from quail medullary cones; long (L, open reading frames) and short (S) cDNA encoded 335 (qAQP4-L) and 301 (qAQP4-S) amino acids with, respectively, 80% and 87% identity to human long- and short-form AQP4. qAQP4-S is identical to qAQP4-L from the second initiation site. Both isoforms have two NPA motifs, but lack cysteine at the known mercury-sensitive site. qAQP4-L and qAQP4-S are expressed in membranes of *Xenopus laevis* oocytes, but both failed to increase the water permeability (P_f) of oocytes exposed to a hypotonic solution. Glutamate (Q242) replacement with histidine did not increase P_f. With conventional RT-PCR and real-time PCR, qAQP4-L/S mRNA signals were detected in the brain, lung, heart, intestine, adrenal gland, skeletal muscle, liver, and kidney (higher in medulla than in cortical region). qAQP4-L mRNAwas detected only in the brain and adrenal gland. Orthogonal arrays of intramembranous particles were not detected in quail CDs. The results suggest that although qAQP4-L and qAQP4-S have high homology to mammalian AQP4, their physiological function may be different.

Keywords

Aquaporin; AQP4; Urine concentration; Medullary collecting duct; *Coturnix quail*; Water channel

1. Introduction

Although avian kidneys can produce hyperosmotic urine by a countercurrent urine concentration system, the ability to form hyperosmotic urine is generally lower in birds than in mammals. Several structural and functional differences exist between avian and mammalian urine-concentrating mechanisms (for review, Schmidt-Nielsen, 1979;Dantzler and Braun, 1980;Nishimura, 1993;Nishimura and Fan, 2002). In avian kidneys, nephrons in the medullary zone have a loop of Henle, whereas loopless nephrons are present in the cortical superficial zone. Also, the thick limb of looped nephrons starts prior to the hairpin turn, and looped nephrons lack the thin ascending limb; thus, avian kidneys lack the inner medulla. We reported previously that arginine vasotocin (AVT; avian antidiuretic hormone) slightly but significantly increases diffusional water permeability (P_f) of the medullary collecting duct (CD) from Japanese quail, *Coturnix coturnix*, via a cAMP mechanism (Nishimura et al., 1996). Recently, we cloned and identified the molecular structure of an AQP2 homologue (qAQP2) water

☆This paper was presented in Experimental Biology's Annual Meeting at San Diego, CA, April 2–6, 2005.

* Corresponding author. Tel.: +1 901 448 5132; fax: +1 901 448 7126. *E-mail address:* nishimur@physio1.utm.edu (H. Nishimura).

channel from medullary cones of the quail kidney (Yang et al., 2004). Immunoreactive qAQP2 is expressed in the apical and subapical regions of cortical and medullary CD cells; expression is higher in the medullary zone.

The AQPs that transport water across the basolateral plasma membrane, however, have not been identified in avian kidneys. In mammalian kidneys, water exits across the basolateral membrane of the CD via AQP3 (Ecelbarger et al., 1995) and/or AQP4 (Terris et al., 1995). We therefore aimed to: 1) identify the cDNA from medullary cones of *Coturnix* quail that encodes AQP proteins other than qAQP2, using a polymerase chain reaction (PCR)-based cloning method and degenerate primers constructed on the basis of the conserved AQP sequences; and 2) investigate whether the identified clones exhibit water channel function when expressed in a *Xenopus laevis* oocyte expression system. AQPs are evolutionarily old water-selective membrane channel proteins found in mammals, plants, and yeasts (Yamamoto and Sasaki, 1998;Agre, 2000;Nielsen et al., 2002). To date, 13 members of the AQP family have been identified in mammals, and at least eight of them are expressed in kidneys (Verkman, 2005). The molecular characterization of avian renal AQPs, however, is currently incomplete.

2. Materials and methods

2.1. Animals and maintenance

Fertilized eggs from Japanese quail, *C. coturnix*, were purchased from G.Q.F. Manufacturing (Savannah, GA, USA) and incubated for 17 days in our laboratory at 37 °C with 60% humidity (80% humidity 3 days before hatching). Hatched birds were fed Game Bird Startena (Purina Mills, Inc.; St. Louis, MO, USA; protein content, 30%) for 2 weeks, and then Chick Start and Grow (Purina; protein content, 17%). Drinking water containing multiple vitamins (G.Q.F. Manufacturing) was given for the first 3 weeks, followed by tap water ad libitum. The photoperiod (10 h light–14 h dark cycle) was controlled. Adult female *X. laevis* were purchased from NASCO (Ft. Atkinson, WI, USA), kept in an aquarium (filtered fresh water) in a cold room (18–20 °C), and fed commercial pellets (NASCO).

2.2. cDNA cloning and cDNA constructs

The kidneys were quickly removed from decapitated adult quail of both sexes. Medullary cones were isolated under a dissecting microscope and homogenized on ice 3 times, 10 s each duration, with dial 6 (Polytron, Brinkman; Westbury, NY, USA). The total RNA was extracted from the supernatant using a Trizol reagent (Gibco Life Technologies; Grand Island, NY, USA) or an acid guanidinium-phenolchloroform extraction method (Chomczynski and Sacchi, 1987) slightly modified for bird tissues (Nishimura et al., 2003;Yang et al., 2004).

After synthesizing first-strand cDNA from the total RNA with a random hexamer primer, the expected AQP-related fragment was amplified with an AdvanTaq PCR Kit (Clontech Lab; Palo Alto, CA, USA) with a pair of degenerate primers selected from two conserved regions of the major intrinsic protein (MIP) family (Fushimi et al., 1993;Yang et al., 2004). The fragment of the expected size (~ 370 bp) was subcloned into a PCR 2.1 T/A-vector (Invitrogen Life Tech.; Carlsbad, CA, USA), and individual clones were further screened by PCR with T7 and M13 reverse primers (Yang et al., 2004). Clones yielding a PCR fragment of ~ 570 bp were selected for sequencing. After identification of the cDNA segment according to known AQP4 sequences, the sequence was extended in the 3′ and 5′ directions using a rapid amplification of cDNA ends (RACE) kit (BD SMART RACE cDNA Amplification kit; BD Biosciences; Palo Alto, CA, USA) with gene-specific primers (GSP) designed from the identified sequence of the cDNA segments, GSP2 (5′-GCCTCGCCAAGTCGGTCTTCTACA-3′) and GSP1 (5′-ACTCGGTGGTGTGATGAGGTAGAGGA-3′), respectively. The RACE products were subcloned into the PCR4-TOPO vector with a T/A cloning kit (Invitrogen) for sequencing (Davis Sequencing LC; Davis, CA, USA). After characterizing the RACE products, the longest and shortest fulllength cDNAs were generated with the extreme 5′end primer (5′-TGAAGCTTCACATGATCG-3′or 5′-GCAAGCTTGAAAACATCATG-3′) and the 3′ end primer (5′-AGTGCCCCGGGCTAGT-3′) (engineered *Hind III* and *Sma I* restriction sites are underlined). The longest full-length cDNA was termed qAQP4-long form (qAQP4-L), and the shortest one was called qAQP4-short form (qAQP4-S).

For cDNA transcription in vitro, qAQP4-L and qAQP4-S cDNA with *Hind III* and *Sma I* restriction sites were subcloned into the pBluescript II SK (−) vector (Stratagene; La Jolla, CA, USA, USA), which contains an upstream *Xenopus* beta-globin enhancer sequence (Preston et al., 1992). Also, to determine whether qAQP4 protein is expressed in oocyte membranes, the pBluescript II SK (−) vector was reconstructed by inserting 10 amino acids of the human c-*myc* epitope (EQKLISEEDL, nucleotides GAACAAAAGCTGATTTCTGAAGAAGACCTG) (Evan et al., 1985) at the *Cla I* multiple cloning site. Tagged qAQP4 cDNAs were prepared by PCR using the following primers: for qAQP4-L, 5′-GAAGCTTATGATCGCAAATGACCCGCGGCTC-3′; for qAQP4-S, 5′-GAAGCTTATGGTAGCATTCAAAGGA-3′; common primer of C-terminus: 5′-AAGACAGAAGACATACTGGGCCCCG-3′.

We compared the qAQP4 amino acid sequence with human, rat, and sheep AQP4 sequences and found that qAQP4 isoforms have glutamine (Q) at site 242 of qAQP4-L and 208 of qAQP4-S, whereas the amino acid in the equivalent position in mammalian AQP4 is histidine (H). To examine whether the amino acid affects water permeability, a mutation of Q208H in the tagged qAQP4-S was constructed by an overlap extension approach (Ho et al., 1989) with 5′-GGGAAATGGGAAAACCACTGG-3′ and 5′-CATCCGGGCAATAGACATAC-3′.All constructs of qAQP4 cDNAs were confirmed by DNA sequence analysis (Davis Sequencing LC, Davis, CA, USA).

2.3. Expression in Xenopus oocytes and measurement of water permeability

To determine whether cloned qAQP4s are water-selective, we measured the osmotic P_f of oocytes injected with the qAQP4 cRNAs transcribed in vitro (Yang et al., 2004). The constructed plasmids were linearized with *Sma I* and transcribed/capped in vitro using T3 polymerase (mMESSAGE Mmachine, Ambio; Austin, TX, USA). Human AQP1 (hAQP1, purchased from American Type Culture Collection (ATCC; Rockville, MD) was used as a positive control (Jung et al., 1994b).

Stage V and VI oocytes from adult female *X. laevis* (NASCO) were injected with 20 nL of solvent (water) or 15–20 ng of cRNA (in 20 nL water) and incubated at 18 °C for 72 h in modified Barth's solution (MBS; 200 mOsmol/kg H_2O) containing 88 mM NaCl, 1.0 mM KCl, 2.4 mM $NaHCO_3$, 15 mM Tris (pH 7.6), 0.3 mM Ca $(NO_3)_2$, 0.4 mM $CaCl_2$, 0.8 mM $MgSO_4$, 100 U/mL penicillin, 100 µg/mL streptomycin, and 0.5 mM theophylline. The MBS was then changed to diluted (70 mOsmol/kg H_2O) MBS, and the time-course change in volume was monitored with a CCD camera (Yang et al., 2004). Osmotic water permeability (P_f) was determined from the initial slope of the time course of $V/V_0[d(V/V_0)/dt]$, initial oocyte volume (V_0=9×10^{-4} cm), initial oocyte surface area (S=0.045 cm^2), the molar volume of water (V_w=18 cm^3/mol), and the osmolarity inside (Osm$_{in}$=200 mOsm) and outside (Osm$_{out}$=70 mOsm) the cell, using the following equation:

$$P_f = [V_0 \times d(V/V_0)/dt] / [S \times V_w \times (\mathrm{Osm}_{in} - \mathrm{Osm}_{out})]$$

(Zhang and Verkman, 1991).

To determine whether qAQP4 cRNA is indeed expressed in oocyte membranes, oocytes injected with *N′*-c-*myc*-qAQP4-L or qAQP4-S cRNAwere fixed in a 3.7% (vol/vol) formaldehyde solution containing 80 mM PIPES, 5 mM Na EGTA, and 1 mM $MgCl_2$, followed by 0.2% (vol/vol) TritonX-100 (Jung et al., 1994b;Yang et al., 2004). The oocytes were incubated with monoclonal anti-mouse c-*myc* antibody (1:100; Sigma–Aldrich; St. Louis, MO, USA) and FITC-conjugated goat anti-mouse IgG (1:250; Chemicon International; Temecula, CA, USA). The bisected oocytes were mounted on 0.5-mm well slides, and fluorescence labeling was examined with a confocal scanning laser microscope (Axiovert200, Carl Zeiss Light Microscopy; Germany).

2.4. Freeze-fracture electron microscopy

We conducted freeze-fracture electron microscopy (modified from Verbavatz et al., 1997;Furman et al., 2003;Silberstein et al., 2004) of CD cell membranes. The kidneys were quickly removed from decapitated quail, and medullary cones were placed in chilled Ringer solution. Two tissue preparations were used: l) dissected medullary cones and 2) single medullary CD dissected under a microscope (Nishimura et al., 1996); several isolated CDs are pooled for fixation. Medullary CDs were identified by location, diameter, and branching; basolateral membrane was identified by location relative to lumen. Both tissue preparations were fixed by immersion in 2% glutaraldehyde/PBS for 2 h at room temperature, washed twice in PBS, and kept in 30%glycerol/PBS (cryoprotection) for 1 h. The samples were mounted (~ 5 μm) on 3-mmcopper freeze-fracture supports and frozen by immersion in liquid N_2-cooled liquid propane. Frozen tubules were fractured with a knife in a fracture apparatus (BAF301, Balzers, Fürstentum Liechtenstein) at −110 °C under 10^{-7} Torr vacuum. A replica of the fractured tubuleswas made by platinumshadowing (~ 1.5-nm coat) at 45 °C, followed by 6 nm of carbon shadowing at 90 °C. The replicas were cleaned in concentrated sodium hypochlorite bleach for several h and with a mixture of chloroform-methanol and water. The replicas were collected on formvar-coated copper grids and examined with an electron microscope (JEOL 2000 EX, JEOL, Japan).

2.5. Reverse transcription polymerase chain reaction (RT-PCR) and quantitative real-time PCR

Conventional RT-PCR and quantitative real-time PCR (QRT-PCR) were used to determine qAQP4 mRNA expression. Total RNA was extracted from the brain, kidney, liver, lung, heart, and skeletal muscle using an acid guanidinium-phenolchloroform method as mentioned above. For conventional RT-PCR, cDNA was reverse-transcribed from total RNA (2.5 μg) with 100 pmol of random hexadeoxynucleotide primer (Pharmacia; Peapack, NJ, USA) in 20 μL of a mixture containing 20 U of RNase inhibitor (Promega; Madison, WI, USA) and 200 U of Moloney Murine Leukemia Virus Reverse Transcriptase (Gibco Life Sci.) in the presence of 50 mM Tris–HCl (pH 8.3), 75 mM KCl, 5.0 mM $MgCl_2$, 1.25 mM dNTP, and 5 mM dithiothreitol (Yang et al., 2004). Double-stranded cDNAs were synthesized and amplified after initial denaturing (94 °C for 5 min) by incubating (total volume, 25 μL in duplicate) the reverse transcription reaction product (3 μL) with 1 U of Taq polymerase (Roche; Mannheim, Germany) and 0.1 μM each of primer, sense primer 5′-GTGACTGTGGCCATGGTCT-3′, and antisense primer 5′-CTTCGTTTTGAATCACAGCTGGC-3′ in the presence of 10 mM Tris–HCl buffer (pH 8.3), 50 mM KCl, 5 mM $MgCl_2$, and 0.35 mM of dNTP for 29 cycles at 94° (denaturation), 60° (primer annealing), and 72 °C (extension/synthesis), respectively, for 30, 30, and 60 s (Yang et al., 2004). PCR using the above primers should yield a 334-bp product and the PCR products presumably detect qAQP4-L/S mRNA. To conduct RT-PCR within the exponential phase of the reaction, the number of cycles, the primer-annealing step, and the polymerization step were optimized (Nishimura et al., 2003;Yang et al., 2004).

For QRT-PCR, reverse transcription reaction was carried out using a Super Script TM First-Strand Synthesis System for RT-PCR kit (Invitrogen Life Tech.). Briefly, 2.5 μg of total RNA were added into 20 μL of final mixture. The mixture was then incubated at 25 °C for 10 min, 42 °C for 50 min, and finally 70 °C for 15 min to stop the reaction. The yields were treated with 1 μL of RNase H for 20 min at 37 °C and stored at −80 °C. QRT-PCR was performed with iCycleriQ (Bio-Rad; Hercules, CA, USA). Amplification of PCR products was monitored via intercalation of SYBR-Green. Primer pairs were designed using Applied Biosystems Primer Express software v. 2.0 (Applied Biosystems; Foster City, CA, USA). The sequences of primer pairs were sense-5′-CTGCAGCGTCTCAAGCTC-3′ and antisense-5′-CACTTGCACAGTCGTCCACA-3′ for detecting qAQP4-L only; sense-5′-AATCAACTGGGGTGGATCAG-3′ and antisense-5′-TTGCAATGCTGAGTCCAAAG-3′, designed to detect qAQP4-L plus qAQP4-S (referred to as qAQP4-L/S); and sense-5′-ATGGCCGTTCTTAGTTGGTG-3′ and antisense-5′-ATGCCAGAGTCTCGTTCGTT-3′ for 18s rRNA as an internal control. cDNAs derived from total RNA were diluted 10 times for qAQP4 and 250 times for 18s rRNA. The PCR mixture contained 1 μL of diluted cDNA, the primer pair mix (2.5 μL 1.0 nM each), and 12.5 μL SYBR Green Master Mix (Applied Biosystems Foster City, CA, USA) in a 25 μL reaction. The PCR conditions include initial denaturation at 95 °C for 10 min, followed by 40 cycles of denaturation at 95 °C for 30 s, annealing at 60 °C for 10 s, and extension at 60 °C for 10 s.

Real-time PCR reactions containing primers for 18s rRNA were also performed in separated wells at the same time as the internal control. A control without template and another control without reverse transcription were included. Relative abundance of mRNA expression in each sample was calculated as $2^{-\Delta\Delta C_T}$, where C_T is threshold cycle, $\Delta\Delta C_T$ indicates that ΔC_T ($C_{T\text{–qAQP4-medullary cones}}-C_{T\text{-18s}}$) from the reference medullary cones sample was subtracted from ΔC_T ($C_{T\text{-qAQP4-each tissue type}}-C_{T\text{-18s}}$) obtained from each tissue type (Livak and Schmittgen, 2001).

2.6. Statistical analysis

All the data are shown as means±SE. For statistical analysis, a single- or two-factor analysis of variance (ANOVA) was used, followed by the Tukey HSD unbalanced test when applicable. The difference was considered significant at a *P*-value of less than 0.05.

3. Results

3.1. Cloning and sequencing of quail AQP4 cDNA

From 20 clones, we selected six clones that have a sequence with 89% identity to rat AQP4. Extension of the fragments in the 3′ and 5′ termini using a RACE technique with specific primers revealed two distinct cDNAs: long- and short-5′ RACE that share the same 689-bp fragment of 3′ RACE partial cDNA (Fig. 1). The short and long cDNAs contain an open reading frame of, respectively, 909 bp and 1008 bp, which encodes 301 (referred to as qAQP4-S) and 335 (referred to as qAQP4-L) amino acids.

qAQP4-S is identical to qAQP4-L from the second initiation site. The alignment of the qAQP4 amino acid sequence with the human AQP4 indicates that qAQP4-L has 80% identity with human AQP4-L (GenBank access number AAC52112), whereas qAQP4-S has 87% identity with human AQP4-S (GenBank access number AAC50284) (Fig. 1-A). The N-terminus of qAQP4-L is shorter in quail (335 amino acids) than in human AQP4-L (341 amino acids), whereas qAQP4-S is equivalent to the human AQP4 short isoform (301 amino acids). qAQP4-S and qAQP4-L contain two NPA motifs that are conserved among MIP family members. Residue 222 of qAQP4-L or 188 of qAQP4-S, corresponding to the mercury-sensitive residue C189 of AQP1, is alanine instead of cysteine. Both qAQP4-S and qAQP4-L contain one putative *N*-linked glycosylation site and five consensus phosphorylation sites (Fig. 1-A). Hydropathic analysis of the translated protein suggests the existence of six putative alpha-helical transmembrane domains (Fig. 1B).

3.2. Membrane expression of qAQP4

We investigated whether *N′*-tagged qAQP4 fusion protein is expressed on the membrane of the oocytes into which *N′*-c-*myc*-qAQP4-L or *N′*-c-*myc*-qAQP4-S cRNA was injected. Intense fluorescent labeling was seen on the plasma membrane of the treated oocytes (Fig. 2A, 2B), whereas no staining was seen on the membrane of the oocytes receiving a water injection (Fig. 2C).

3.3. Effect on Xenopus oocyte water permeability

First, we determined the time courses of volume changes and osmotic P_f of oocytes injected with WT-qAQP4s or *N′*-c-*myc*-qAQP4s. No difference was seen in the P_f of the oocytes from these two groups (data not shown); hence, only the volume changes and P_f of the oocytes injected with *N′*-c-*myc*-qAQP4 cRNAs are shown (Fig. 3A, 3B). Following exposure to hypoosmotic (70 mOsm) MBS, the oocytes injected with hAQP1 (positive control) swelled profoundly within 3 min, whereas those injected with *N′*-c-*myc*-qAQP4 cRNAs showed only modest swelling that was not significantly different from that of the control (injected with water) at each time point. The P_f (10^{-4} cm/s) of the oocytes treated with hAQP1 cRNA (20 ng) (155.1±12.2) was more than 20 times higher than that of the water control (7.4±1.4). The P_f of the oocytes treated (20 ng) with *N′*-c-*myc*-qAQP4-S (13.5±2.1) or *N′*-c-*myc*-qAQP4-L cRNA (12.7±1.2) was not significantly different from that of the control (Fig. 3B). The P_f of the oocytes injected with *N′*-c-*myc*-qAQP4-S Q242H (16.8±2.3) was not significantly different from that of qAQP4-L or qAQP4-S, although it was slightly higher than that of the water control (Fig. 3B). Preincubation with 0.3 mM $HgCl_2$ for 5 min did not significantly alter the P_f of the oocytes.

3.4. Tissue-specific expression of qAQP4 mRNA and quantitative real-time PCR

Conventional RT-PCR—The tissue distribution of qAQP4 mRNA determined by conventional RT-PCR with specific primers is shown in Fig. 4A. The RT-PCR products of total RNA extracted from the brain, kidney, lung, and skeletal muscle exhibited a single 334-bp band. This fragment matches the expected size of qAQP4. The densities of RT-PCR products (qAQP-L/S mRNA) are higher in the brain and kidney than in the lung and skeletal muscle (Fig. 4A). No RT-PCR products were detected in the liver or heart.

Quantitative real-time PCR (QRT-PCR)—The tissue distribution and relative levels of qAQP4 mRNA determined by QRT-PCR with specific primers are shown in Fig. 4B and Table 1. The qAQP4-L/S mRNA signal was detected in the lung, heart, liver, skeletal muscle, brain, intestine, adrenal gland, and kidney. Relative levels of qAQP4-L/S mRNA (subtracting ΔC_T-medullary cones from Δ C_T [$C_{T\text{-organ}}$–$C_{T\text{-18s}}$] of each organ, see methods) were highest in the brain and adrenal gland (Fig. 4B and Table 1). The level of qAQP4-L/S mRNA was higher in the medullary cones than in the superficial zone of the kidney (Fig. 4B). The qAQP4-L mRNA signal was detected only in the brain and adrenal gland (Table 1).

3.5. Freeze-fracture electron microscopy of isolated CD membrane

Freeze-fracture electron microscopic analysis of CD cell membranes is shown in Fig. 5. Clusters of intramembranous particles are seen in the basolateral membranes of mucus-secreting epithelial cells (equivalent to principal cells of mammalian kidney) of the CD, but orthogonal array arrangement was not noted. For contrast, protoplasmic (P)-face views of basolateral membranes of mouse medullary CDs are also shown in Fig. 5. In general, particles are slightly smaller than those in rat AQP4 (Verbavatz et al., 1997).We examined kidney slices and isolated tubules collected from two adult quail.

3.6. Phylogenetic analysis of qAQPs

Amino acid sequences were aligned using the default options of a Clustal X program (version 1.83), and the resulting multiple alignments were refined by visual inspection. Neighbor-joining (NJ) analysis (Saitou and Nei, 1987) of the amino acid alignment was based on mean character distance matrices. AQPs from plants and bacteria were not included in the analysis. A NJ analysis of AQP isoforms shows that members of the AQP family appear to have diverged into three major groups (Fig. 6). The first group (Fig. 6A, upper area) includes aquaglyceroporins that are permeable to both water and glycerol (AQP3, 7, 9, and 10). The second group (Fig. 6A, middle area) includes AQP0, 2, 5, and 6 and their isoforms. Within the second group, the branch leading to AQP2 and AQP5 evolved later than the branch leading to AQP0 isoforms. The third group (Fig. 6A. lower area) shows two clusters, AQP1 and AQP4, although the homology of these groups is only 48%. Overall, the evolutionary lines leading to AQP1 and AQP4 appear to have diverged phylogenetically earlier than those leading to AQP2. The phylogenetic tree of aquaporin superfamily drawn by the same program is shown in Fig. 6B.

4. Discussion

AQPs are a family of small, hydrophobic proteins (major intrinsic protein, MIP) that were originally cloned in mammalian lens as MIP26 (for review, Yamamoto and Sasaki, 1998;Borgnia et al., 1999;Agre, 2000). Two major subgroups (AQP and aquaglyceroporin) have been identified. AQPs are phylogenetically old, and DNA sequences encoding AQP proteins have been found throughout nature (Borgnia et al., 1999). In the present study, we have identified two distinct polypeptide amino acid sequences that differ in length at the N-terminus. The sequence of qAQP4-S (301 amino acids) is the same as that of qAQP4-L (335 amino acids) except that the former lacks 34 amino acids at the N-terminus. Both qAQP4-L and qAQP4-S contain two NPA motifs between transmembrane domains (TMD) 2–3 (loop B) and TMD 5–6 (loop E). Loops B and E are significantly hydrophobic, with high homology to human AQP4 (80% and 87% identity, respectively, to human long-and short-form AQP4). The presence of two different lengths of qAQP4 cDNAs encoding two distinct polypeptides that differ at the N-terminus suggests that qAQP4 protein isoforms are likely derived from different mRNAs. Using the nucleotide sequence of qAQP4-L as a query, we searched the chicken genome database on NCBI BLAST and found that more than 97% of the qAQP4 sequence is identical to chicken genomic DNA at chromosome locus 2. This sequence appears discontinuously at four different positions of genomic DNA, suggesting that, as reported for human AQP4 (Yang et al., 1995), qAQP4 may be a single copy gene at chromosome locus 2 that encodes protein isoforms that are ascribed to the transcripts generated by alternative splicing.

Unlike rat AQP4 (Yang and Verkman, 1997) or human AQP4 (Yang et al., 1995), however, neither qAQP4-L nor qAQP4-S significantly increases the P_f of *X. laevis* oocytes, suggesting that qAQP4 does not function as a water channel. We confirmed that qAQP4 proteins are expressed on the membrane of *Xenopus* oocytes. We reached this conclusion based on the following evidence. First, it is unlikely that an incorrect sequence of qAQP4 accounts for the lack of water channel function. The qAQP4-L cloned in two separate experiments from different quail exhibited an identical coding sequence (GenBank access No. AF465730, 2002), and both clones showed no stimulation of water permeability in the *Xenopus* oocyte expression system. To further eliminate the possibility that we had identified an incorrect sequence, we repeated the cloning of qAQP4-L with specific gene primers (see Materials and methods) and

NIH-PA Author Manuscript

NIH-PA Author Manuscript

obtained the same sequences as with the qAQP4-L cDNA. Second, the technical pitfalls of using a *Xenopus* oocyte expression system can be precluded because the hAQP1-expressing oocytes, used as a positive control, consistently exhibit potent water permeability. Third, it is unlikely that the failure to exhibit water permeability is due to the vector, since the same vector as that of hAQP1, containing an upstream *Xenopus* beta-globin enhancer sequence, was used in the constructions. Fourth, we demonstrated that *N′*-c-*myc*-qAQP4 is expressed in *Xenopus* oocyte membranes. Therefore, the low P_f is likely to be an intrinsic property of qAQP4.

Because avian urine is usually acidic but variable, with a pH range of 5–8 (Long and Skadhauge, 1983), we examined whether qAQP4's water channel activity may vary depending on environmental pH. It has been reported that the water and glycerol permeability of mammalian AQP3 is higher in acidic pH (pH 6.1–6.4) (Zeuthen and Klaerke, 1999). We therefore examined the relationship between the pH of the Barth's solution and the P_f. The oocyte membrane in which qAQP4 S/L is expressed failed, however, to increase P_f at either pH 6.0 or pH 8.5 (data not shown). We also found that qAQP4-L (Q242) and qAQP4-S (Q208) are distinctly different from qAQP2 and mammalian AQPs 1, 2, and 4 that have a histidine (H) at the equivalent location. Hence, we determined whether replacement of glutamine with histidine (Q208H) in qAQP4-S enhances P_f when expressed in *Xenopus* oocytes. The P_f of Q208H cRNA-expressed membrane remained low, suggesting that the lack of histidine (208) in qAQP4 is unlikely to be important for water permeability.

In mammalian AQP4, enhancement of water permeability is not inhibitable by $HgCl_2$ (Jung et al., 1994a), presumably due to the lack of a mercury-sensitive site (cysteine at 189 of AQP1; Preston et al., 1993). Likewise, qAQP4 (both L and S) lacks cysteine at G106 or A222, and $HgCl_2$ did not alter the P_f of qAQP4-expressed oocytes. It has been shown that $HgCl_2$ enhances the P_f of AQP6- (Yasui et al., 1999) and AQPxlo-expressed (Virkki et al., 2002) oocytes.

In humans, AQP4 mRNA is detectable in the brain, muscle, heart, kidney, and lung (Yang et al., 1995). Likewise, we detected qAQP4-L/S mRNA in the brain, kidney, lung, and skeletal muscle by conventional RT-PCR, and in the liver, heart, adrenal gland, and intestine by real-time PCR. The levels of qAQP4-L/S mRNA in the adrenal gland and brain are higher than in other tissues, whereas qAQP4-L mRNA is detectable only in the brain and adrenal gland. Although we could not directly compare expression levels of the two forms, it appears that the expression level of qAQP4-S mRNA may be higher than that of qAQP4-L. First, the C_T values of qAQP4 are ~ 30 and ~ 33 in the brain and adrenal gland, respectively, whereas the C_T values for qAQP4-L/S are ~ 21 and ~ 23. SYBR green is a fluorogenic minor groove-binding dye that emits a strong fluorescent signal upon binding to double-stranded DNA (Morrison et al., 1998). Thus, the higher the initial amount of the first single cDNA, the sooner the accumulated product is detected in the PCR (hence, C_T is low), suggesting that the PCR product, presumably the mRNA level, is higher in qAQP4-S. Second, qAQP4-L/S mRNA signals, but not qAQP4-L mRNA signals, are detectable by real-time PCR in the liver, lung, muscle, intestine, kidney, and heart. In rats, rAQP4 is also expressed in two isoforms that differ at their N termini: isoforms in which translation initiation occurs at the first methionine (referred to as M1) and at the second methionine (referred to as M23). Both isoforms are present in the brain, but the expression of M23 is at least three times greater than that of M1 (Neely et al., 1999).

Madrid et al. (2001) identified in epithelial MDCK (Madin–Darby canine kidney) cells two independent C-terminal signals that regulate a sorting of AQP4 molecules from the Golgi apparatus to the basolateral membrane: 1) a signal that encodes a dileucine-like motif preceded by a cluster of acidic residues (ETEDLIL) and 2) a signal consisting of a tyrosine-based motif (GSYMEV). The latter also appears to regulate AQP4 endocytosis and cell surface expression through serial interactions with different clathrin-adaptor protein complexes. Mutation of these motifs significantly impairs basolateral targeting of AQP4 (Madrid et al., 2001). In contrast, the two motifs in the equivalent positions in qAQP4 are ETDDLIL and GKYIEV, respectively. It is of interest to investigate whether alteration in these sequences impairs basolateral sorting and expression of qAQP4, leading to the lack of water channel function.

Furthermore, orthogonal arrays of intramembranous particles (OAPs) arranged in what appears to be an AQP4-specific membrane organization have been reported in the CD cells from intact mice (Verbavatz et al., 1997), Chinese hamster ovary (CHO) cells transfected with AQP4 (Furman et al., 2003;Yang et al., 1996) and principal cells of CDs from Brattleboro rats that lack ADH (Silberstein et al., 2004). These OAPs are not seen in transgenic mouse lacking AQP4, suggesting that OAP protein is likely to be AQP4 (Verbavatz et al., 1997). Although the function of OAP is not yet understood, this intramembrane organization may enhance osmotic water permeability (Silberstein et al., 2004). Freeze-fracture micrograph images of CHO cells transfected with M23 show large, raft-like square arrays (>100 particles/array), whereas square arrays in M1-transfected cells are much smaller (2–12 particles/array) (Furman et al., 2003). Interestingly, the expression ratio between the long and short forms of the AQP4 splicing variants may determine the size of the orthogonal arrays and influence cell adhesion via AQP molecules in adjacent cells (Hiroaki et al., 2006). Freeze-fracture electron microscopy analysis of isolated medullary CD cell membranes from Japanese quail showed diffuse intramembranous particles on the basolateral membrane (protoplasmic face) but no orthogonal array arrangements were seen. This finding supports the absence of water channel activity of qAQP4.

We have previously shown that in isolated CDs perfused in vitro, diffusional water permeability (measured with tritiated water) is considerable and is increased in hyperosmotic media or by serosal application of vasotocin (Nishimura et al., 1996). Furthermore, the apical membrane of the CD expresses the AQP2 water channel, which is enhanced by endogenously released or exogenously applied vasotocin (Yang et al., 2004). In rats, AQP4 and AQP3 are constitutively expressed on the basolateral membrane of the CD principal cells in the inner medulla and outer/inner medulla, respectively, of the kidney and represent the pathway for water exit (Terris et al., 1995;Ecelbarger et al., 1995). It is therefore necessary to examine whether the AQP3 homologue water channel may be expressed in the basolateral membrane of CD cells of the quail responsible for water exit.

Although it is anticipated that all vertebrate kidneys possess AQPs, AQP homologue molecules have been cloned from only a limited number of species of non-mammalian vertebrates (Zardoya and Villalba, 2001;Nishimura and Fan, 2002,2003; and Fig. 6). The AQP1 homologue cloned from Japanese eels has two isoforms; short- and long-form AQP1 are expressed predominantly in the intestine and are upregulated in seawater (Aoki et al., 2003). Two AQP homologue cDNAs that have considerable homology to AQP1 have been cloned from amphibian urinary bladders: 1) AQP-toad bladder (AQP-TB; Siner et al., 1996) and 2) frog AQP-CHIP (FA-CHIP; Abrami et al., 1994). ADH-elicited water channels in the *Hyla* tree frog skin, AQP-h2 and AQP-h3, have been identified by Tanii et al. (2002) and Hasegawa et al. (2003), but their homology to AQP2 is rather low. More recently, an AQP2-like water channel with high homology to mammalian AQP2 has been cloned from the *Hyla* tree frog (GenBank access No. ABC98209). ADH-sensitive AQP2 is found in Japanese quail (Yang et al., 2004). AQP3 homologue mRNA is expressed in the gill, esophagus, and rectal tissues of European eels (Lignot et al., 2002), and an AQP homologous to MIP 26 has been cloned from the eye lens of killifish (Virkki et al., 2001).

Full-length AQP4 (97% homology to qAQP4) that encodes 335 predicted amino acids has been identified in chickens (Saito et al., 2005). Chicken AQP4 (cAQP4) mRNA was increased in the brain and decreased in the kidney by water deprivation; the physiological significance of these effects, however, remains to be clarified. AQP4 homologue cloned from marine hagfish

NIH-PA Author Manuscript

NIH-PA Author Manuscript

(*Eptatretus burgeri*; ebAQP4) has a modest (~ 40%) identity to mammalian AQP4 (Nishimoto et al., 2006) and is expressed only in the gills; when it is expressed, P_f increases. In the phylogenetic tree shown in Fig. 6, ebAQP4 is somewhat distant from the AQP4 cluster, whereas qAQP4 and rAQP4 are closely linked. Zardoya and Villalba (2001) conducted comprehensive phylogenetic analysis of AQPs (defined as a family of MIPs that have a water channel function) to identify homologous groups (orthologues and paralogues). Water channel proteins are classified into six major paralogous groups in which vertebrate AQPs belong to either group 1, glycerol-transporting proteins, or group 2, AQPs that regulate water transport in specialized tissues. The most basal orthologue in this group is AQP4, and the next gene duplication gave rise to AQP1, which is a highly ubiquitous water channel protein, and to the ancestor of a group of tissue-specific AQPs that includes AQP0, AQP6, AQP2, and AQP5. The latter two appear to be the most recent duplications within the AQP gene family (Zardoya and Villalba, 2001). This evolutionary analysis agrees with the order of appearance of AQPs within the phylogenetical advancement of vertebrates that we discussed above.

In summary, we have identified two isoforms of qAQP4 cDNA (qAQP4-L and qAQP4-S) from quail medullary cones that differ at the N-terminus. While qAQP4-S is expressed in various tissues, qAQP-L is primarily seen in the brain and adrenal glands. qAQP4-L mRNA and qAQP4-S mRNA expressed in *X. laevis* oocytes, however, did not enhance water permeability, suggesting that, despite qAQP4's high homology to mammalian AQP4, the intrinsic function of qAQP4 may be different. More recent studies suggest that, in addition to fluid transport function, AQPs may have a role in cell migration, lipid metabolism, and neural signal transudation (Verkman, 2005). Such possibilities remain to be explored in bird kidneys.

Acknowledgements

The authors are grateful for support by NSF grant IBN-9986633 and IOB0615359, and NIH grant HL52881 (PI: Hiroko Nishimura), and by NIH grantsMG61943 and HL58133 (PI: Zheng Fan). We thank Dr. Sei Sasaki, Tokyo Medical and Dental University, Japan, for his helpful advice; Dr. Peter Agre, Johns Hopkins University, for his generous gift of AQP plasmid; and Dr. Jonathan Kyle, University of Chicago, for kindly helping us in some of the experiments. We also thank Ms. Ping Jiao and Ms. Jessica Bolen for their excellent technical assistance.

References

Abrami L, Simon M, Rousselet G, Berthonaud V, Buhler JM, Ripoche P. Sequence and functional expression of an amphibian water channel, FACHIP: a newmember of theMIP family. Biochim Biophys Acta 1994;1192:147–151. [PubMed: 7515688]

Agre P. Aquaporin water channels in kidney. J Am Soc Nephrol 2000;11:764–777. [PubMed: 10752537]

Aoki M, Kaneko T, Katoh F, Hasegawa S, Tsutsui N, Aida K. Intestinal water absorption through aquaporin 1 expressed in the apical membrane of mucosal epithelial cells in seawater-adapted Japanese eel. J Exp Biol 2003;206:3495–3505. [PubMed: 12939380]

Borgnia M, Nielsen S, Engel A, Agre P. Cellular and molecular biology of the aquaporin water channels. Annu Rev Biochem 1999;68:425–458. [PubMed: 10872456]

Chomczynski P, Sacchi N. Single-step method of RNA isolation by acid guanidinium thiocyanate-phenol-chloroform extraction. Anal Biochem 1987;162:156–159. [PubMed: 2440339]

Dantzler WH, Braun EJ. Comparative nephron function in reptiles, birds, and mammals. Am J Physiol 1980;239:R197–R213. [PubMed: 7001920]

Ecelbarger CA, Terris J, Frindt G, Echevarria M, Marples D, Nielsen S, Knepper MA. Aquaporin-3 water channel localization and regulation in rat kidney. Am J Physiol 1995;269:F663–F672. [PubMed: 7503232]

Evan GI, Lewis GK, Ramsay G, Bishop JM. Isolation of monoclonal antibodies specific for human c-myc proto-oncogene product. Mol Cell Biol 1985;5:3610–3616. [PubMed: 3915782]

Furman CS, Gorelick-Feldman DA, Davidson KG, Yasumura T, Neely JD, Agre P, Rash JE. Aquaporin-4 square array assembly: opposing actions ofM1 and M23 isoforms. Proc Natl Acad Sci U S A 2003;100:13609–13614. [PubMed: 14597700]

Fushimi K, Uchida S, Hara Y, Hirata Y, Marumo F, Sasaki S. Cloning and expression of apical membrane water channel of rat kidney collecting tubule. Nature 1993;361:549–552. [PubMed: 8429910]

Hasegawa T, Tanii H, Suzuki M, Tanaka S. Regulation of water absorption in the frog skins by two vasotocin-dependent water-channel aquaporins, AQP-h2 and AQP-h3. Endocrinology 2003;144:4087–4096. [PubMed: 12933683]

Hiroaki Y, Tani K, Kamegawa A, Gyobu N, Nishikawa K, Suzuki H, Walz T, Sasaki S, Mitsuoka K, Kimura K, Mizoguchi A, Fujioshi Y. Implications of the aquaporin-4 structure on array formation and cell adhesion. J Mol Biol 2006;355:628–639. [PubMed: 16325200]

Ho SN, Hunt HD, Horton RM, Pullen JK, Pease LR. Site-directed mutagenesis by overlap extension using the polymerase chain reaction. Gene 1989;77:51–59. [PubMed: 2744487]

Jung JS, Bhat RV, Preston GM, Guggino WB, Baraban JM, Agre P. Molecular characterization of an aquaporin cDNA from brain: candidate osmoreceptor and regulator of water balance. Proc Natl Acad Sci U S A 1994a;91:13052–13056. [PubMed: 7528931]

Jung JS, Preston GM, Smith BL, Guggino WB, Agre P. Molecular structure of the water channel through aquaporin CHIP. The hourglass model J Biol Chem 1994b;269:14648–14654.

Lignot JH, Cutler CP, Hazon N, Cramb G. Immunolocalisation of aquaporin 3 in the gill and the gastrointestinal tract of the European eel *Anguilla anguilla* (L.). J Exp Biol 2002;205 (Part 17):2653–2663. [PubMed: 12151371]

Livak KJ, Schmittgen TD. Analysis of relative gene expression data using real-time quantitative PCR and the $2^{-\Delta\Delta C_T}$ method. Methods 2001;25:402–408. [PubMed: 11846609]

Long S, Skadhauge E. Renal acid excretion in the domestic fowl. J Exp Biol 1983;104:51–58. [PubMed: 6409979]

Madrid R, Le Maout S, Barrault MB, Janvier K, Benichou S, Merot J. Polarized trafficking and surface expression of the AQP4 water channel are coordinated by serial and regulated interactions with different clathrin-adaptor complexes. EMBO J 2001;20:7008–7021. [PubMed: 11742978]

Morrison TB, Weis JJ, Wittwer CT. Quantification of low-copy transcripts by continuous SYBR Green I monitoring during amplification. Biotechniques 1998;24:954–958. [PubMed: 9631186]

Neely JD, Christensen BM, Nielsen S, Agre P. Heterotetrameric composition of aquaporin-4 water channels. Biochemistry 1999;38:11156–11163. [PubMed: 10460172]

Nielsen S, Frokiaer J, Marples D, Kwon TH, Agre P, Knepper MA. Aquaporins in the kidney: from molecules to medicine. Physiol Rev 2002;82:205–244. [PubMed: 11773613]

Nishimoto G, Sasaki G, Yaoita E, Nameta M, Li H, Furuse K, Fujinaka J, Yoshida Y, Yamamoto T. Molecular characterization of water selective AQP, EbAQP4, in a hagfish: Insight into ancestral form of AQP4. Am J Physiol 2006;292:R644–R651.

Nishimura, H. Countercurrent urine concentration in birds. In: Brown, JA.; Balment, RJ.; Rankin, JC., editors. New Insight inVertebrate Kidney Function, Society for Experimental Biology Seminar Series. 52. Cambridge Univ. Press; Cambridge: 1993. p. 189-212.

Nishimura, H.; Fan, Z. Sodium and water transport and urine concentration in avian kidney. In: Hazon, N.; Flik, G., editors. Osmoregulation and Drinking in Vertebrates. BIOS Scientific Publishers Ltd; Oxford: 2002. p. 129-151.

Nishimura H, Fan Z. Regulation of water movement across vertebrate renal tubules. Comp Biochem Physiol A 2003;136:479–498.

Nishimura H, Koseki C, Patel TB. Water transport in collecting ducts of Japanese quail. Am J Physiol 1996;271:R1535–R1543. [PubMed: 8997350]

Nishimura H, Yang Y, Hubert C, Gasc JM, Ruijtenbeek K, De Mey J, Struijker-Boudier HAJ, Corvol P. Maturation-dependent changes of angiotensin receptor expression in fowl. Am J Physiol 2003;285:R231–R242.

Preston GM, Carroll TP, Guggino WB, Agre P. Appearance of water channels in *Xenopus* oocytes expressing red cell CHIP28 protein. Science 1992;256:385–387. [PubMed: 1373524]

Preston GM, Jung JS, Guggino WB, Agre P. The mercury-sensitive residue at cysteine 189 in the CHIP28 water channel. J Biol Chem 1993;268:17–20. [PubMed: 7677994]

Saito N, Ikegami H, Shimada K. Effect of water deprivation on aquaporin 4 (AQP4) mRNA expression in chickens (*Gallus domesticus*). Mol Brain Res 2005;141:193–197. [PubMed: 16246454]

Saitou N, Nei M. The neighbor-joining method: a new method for reconstructing phylogenetic trees. Mol Biol Evol 1987;4:406–425. [PubMed: 3447015]

Schmidt-Nielsen B. Urinary concentrating processes in vertebrates. Yale J Biol Med 1979;52:545–561. [PubMed: 538955]

Silberstein C, Bouley R, Huang Y, Fang P, Pator-Soler P, Brown D, Van Hoek AN. Membrane organization and function of M1 and M23 isoforms of aquaporin-4 in epithelial cells. Am J Physiol 2004;287:F501–F511.

Siner J, Paredes A, Hosselet C, Hammond T, Strange K, Harris HW. Cloning of an aquaporin homologue present in water channel containing endosomes of toad urinary bladder. Am J Physiol 1996;270:C372–C381. [PubMed: 8772465]

Tanii H, Hasegawa T, Hirakawa N, Suzuki M, Tanaka S. Molecular and cellular characterization of a water-channel protein, AQP-h3, specifically expressed in the frog ventral skin. J Membr Biol 2002;188:43–53. [PubMed: 12172646]

Terris J, Ecelbarger CA, Marples D, Knepper MA, Nielsen S. Distribution of aquaporin-4 water channel expression within rat kidney. Am J Physiol 1995;269:F775–F785. [PubMed: 8594871]

Verbavatz JM, Ma T, Gobin R, Verkman AS. Absence of orthogonal arrays in kidney, brain and muscle from transgenic knockout mice lacking water channel aquaporin-4. J Cell Sci 1997;110:2855–2860. [PubMed: 9427293]

Verkman AS. More than just water channels: unexpected cellular roles of aquaporins. J Cell Sci 2005;118:3225–3232. [PubMed: 16079275]

Virkki LV, Cooper GJ, Boron WF. Cloning and functional expression of a MIP (AQP0) homolog from killifish (*Fundulus heteroclitus*) lens. Am J Physiol 2001;281:R1994–R2003.

Virkki LV, Franke C, Somieski P, Boron WF. Cloning and functional characterization of a novel aquaporin from *Xenopus laevis* oocytes. J Biol Chem 2002;277 (43):40610–40616. [PubMed: 12192003]

Yamamoto T, Sasaki S. Aquaporins in the kidney: emerging new aspects. Kidney Int 1998;54:1041–1051. [PubMed: 9767520]

Yang B, Verkman AS. Water and glycerol permeabilities of aquaporins 1–5 and MIP determined quantitatively by expression of epitope-tagged constructs in *Xenopus* oocytes. J Biol Chem 1997;272:16140–16146. [PubMed: 9195910]

Yang B, Ma T, Verkman AS. cDNA cloning, gene organization, and chromosomal localization of a human mercurial insensitive water channel. Evidence for distinct transcriptional units. J Biol Chem 1995;270:22907–22913. [PubMed: 7559426]

Yang B, Brown D, Verkman AS. Themercurial insensitivewater channel (AQP-4) forms orthogonal arrays in stably transfected Chinese hamster ovary cells. J Biol Chem 1996;271:4577–4580. [PubMed: 8617713]

Yang Y, Cui Y, Wang W, Zhang L, Bufford L, Sasaki S, Fan Z, Nishimura H. Molecular and functional characterization of a vasotocin-sensitive aquaporin water channel in quail kidney. Am J Physiol 2004;287:R915–R924.

Yasui M, Hazama A, Kwon TH, Nielsen S, Guggino WB, Agre P. Rapid gating and anion permeability of an intracellular aquaporin. Nature 1999;402:184–187. [PubMed: 10647010]

Zardoya R, Villalba S. A phylogenetic framework for the aquaporin family in eukaryotes. J Mol Evol 2001;52:391–404. [PubMed: 11443343]

Zeuthen T, Klaerke DA. Transport of water and glycerol in aquaporin 3 is gated by H^+ J Biol Chem 1999;274:21631–21636. [PubMed: 10419471]

Zhang R, Verkman AS. Water and urea permeability properties of *Xenopus* oocytes: expression of mRNA from toad urinary bladder. Am J Physiol 1991;260:C26–C34. [PubMed: 1987778]

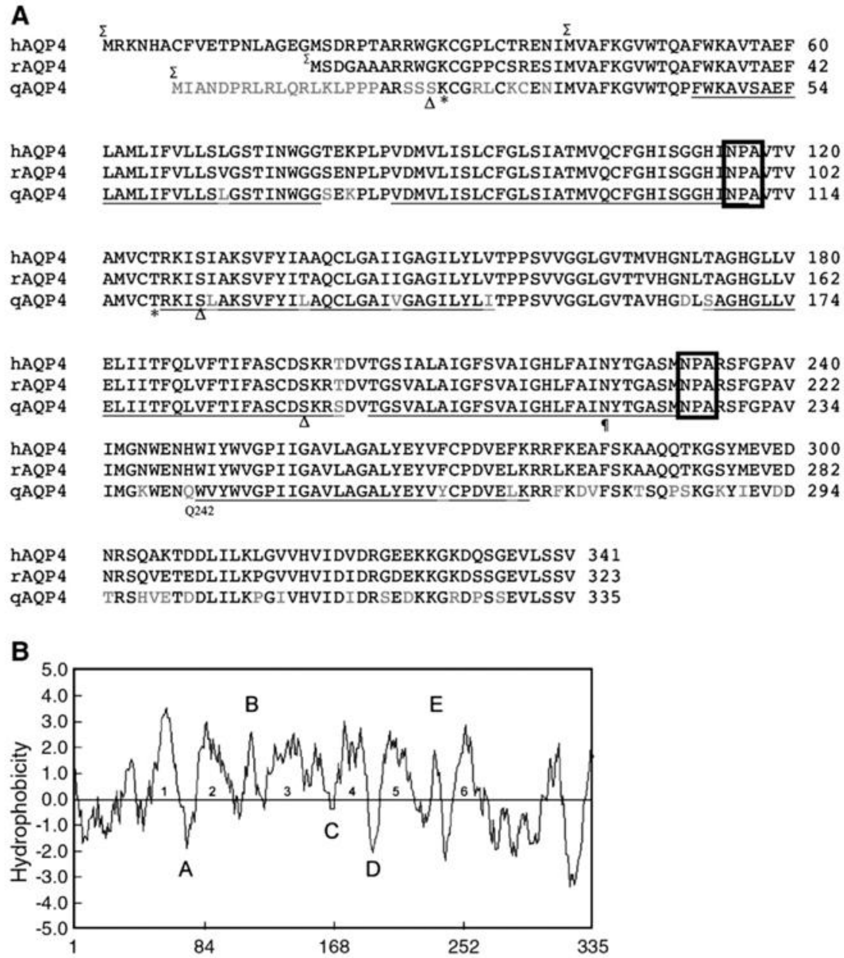

Fig 1.

A: The amino acid sequence of quail AQP4 (qAQP4) compared with human (hAQP4) and rat (rAQP4) water channels. Amino acid residues that match the quail sequence are shown in black, and those not matching it are in gray. Six transmembrane domains are underlined. The water-selective NPA motif is framed in black. Symbols (qAQP4) indicate consensus sites for *N*-linked glycosylation (¶), protein kinase A (▵) and C (*), potential translation initiation sites (Σ), and replacement of glutamine (Q242). B: Hydropathy analysis based on the Kyte–Doolittle algorithm (window size, 7) indicates that qAQP4 spans the membrane six times (1–6) and that its N- and C-termini are located intracellularly. Loops A, C, and E are extracellular; Loops B and D are intracellular.

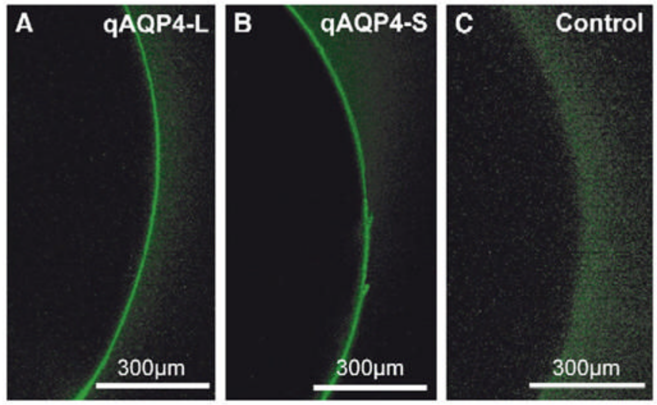

Fig 2.
Immunofluorescence images from oocytes injected with *N′*-c-*myc*-qAQP4 cRNAs. Oocyte membranes were imaged with a confocal scanning laser microscope fitted to a Nikon Optiphot. The oocytes were treated with monoclonal mouse c-*myc* antibody. A (qAQP4-L, long form) and B (qAQP4-S, short form) show that strong surface expression was seen in the plasma membrane of oocytes injected with qAQP4-L and qAQP4-S cRNA, whereas no labeling was seen in control oocytes injected with water (C).

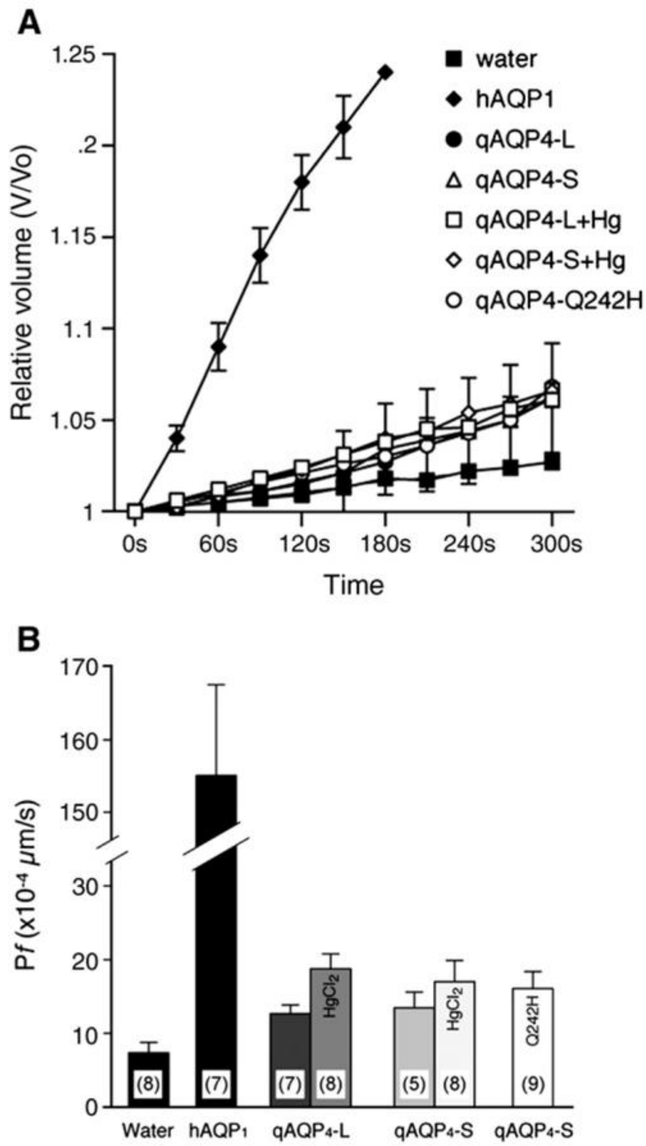

Fig 3.

Osmotic water permeability of *X. laevis* oocytes injected with human aquaporin 1 (hAQP1) cRNA, *N′*-c-*myc*-qAQP4 cRNA, or water (control) and maintained for 72 h. The modified Barth's solution (MBS; 200 mOsm) was changed to 70 mOsm, and the volume of oocytes was monitored with a Nikon phase-contrast microscope. A: Time-course changes of oocyte volumes relative to the volume at time zero (V_0) were examined. The groups treated with 0.3 mM $HgCl_2$ were exposed for 5 min before the start of the time-course experiment. B: Osmotic water permeability coefficients (P_f) were calculated from the time-dependent changes in volume. Values are means±SE. s, second; Numbers of oocytes in columns.

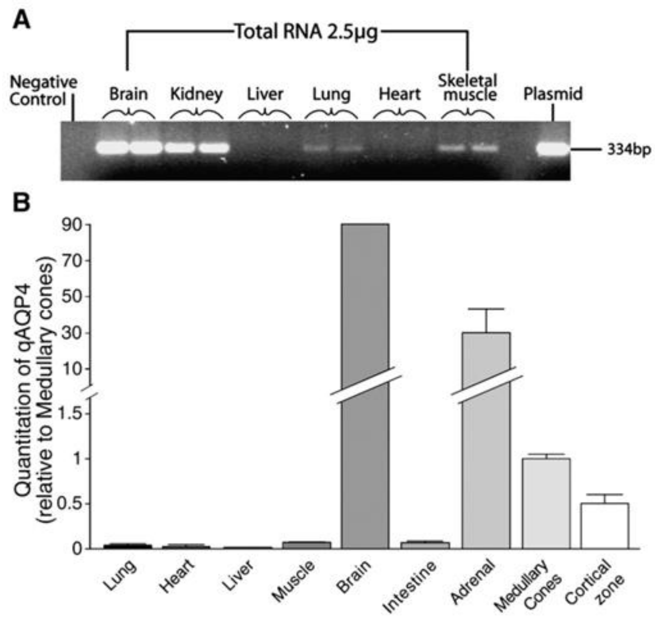

Fig 4.

A: Tissue distribution of qAQP4. Total RNA was extracted from the brain, kidney, lung, liver, heart, and skeletal muscle. RT-PCR products were amplified from total RNA (2.5 μg, duplicate determinations in each tissue) with a pair of primers. The fragment from the RT-PCR products was 334 bp, as expected. All RNA preparations were free from DNA contamination (no band from reverse transcriptase minus incubation). NC: negative control in which the reverse transcription product was deleted from the PCR incubation. Plasmid cDNA containing qAQP4 (~ 30 pg) was used for positive control. B: Tissue-specific expression of qAQP4-L and qAQP4-L/S using quantitative real-time PCR. The relative quantification of qAQP4 mRNA was calculated by the $2^{-\Delta\Delta C_T}$ method. The amount of qAQP4 mRNA is relative to medullary cones. Values are mean±SE.

NIH-PA Author Manuscript

NIH-PA Author Manuscript

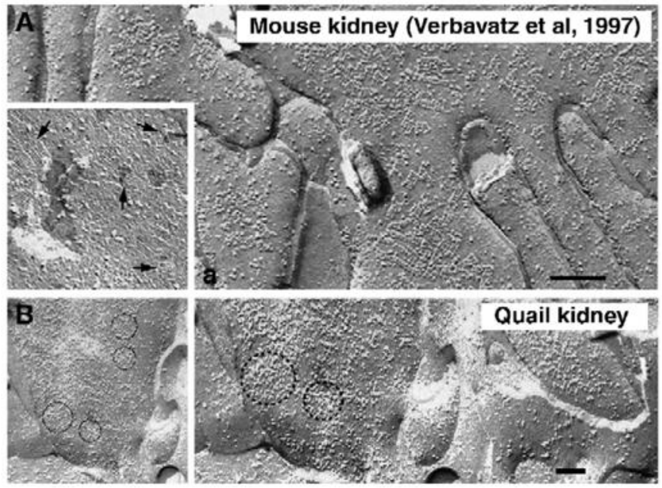

Fig 5.

Freeze-fracture electron microscopy of (A) medullary collecting duct (CD) cells from intact mouse (reproduced with permission from Verbavatz et al., J. Cell Science 110:2855–2860–1997) and (B) medullary CD epithelial cells from quail kidney. Tissue sections were fixed, cytoprotected, freeze-fractured, and replicated with high-resolution shadowing methods. Protoplasmic (P)-face views of basolateral membranes of mouse CD cells show aggregates of intramembranous particles (IMPs) forming orthogonal arrays (A, arrows). Horizontal bar: 150 nm. The P-face of basolateral membranes of medullary CD cells from Japanese quail reveals clusters of IMPs (B, circle), but neither orthogonal arrays nor particle aggregates are noted. Horizontal bar: 100 nm. See Materials and methods for fixation and mounting conditions.

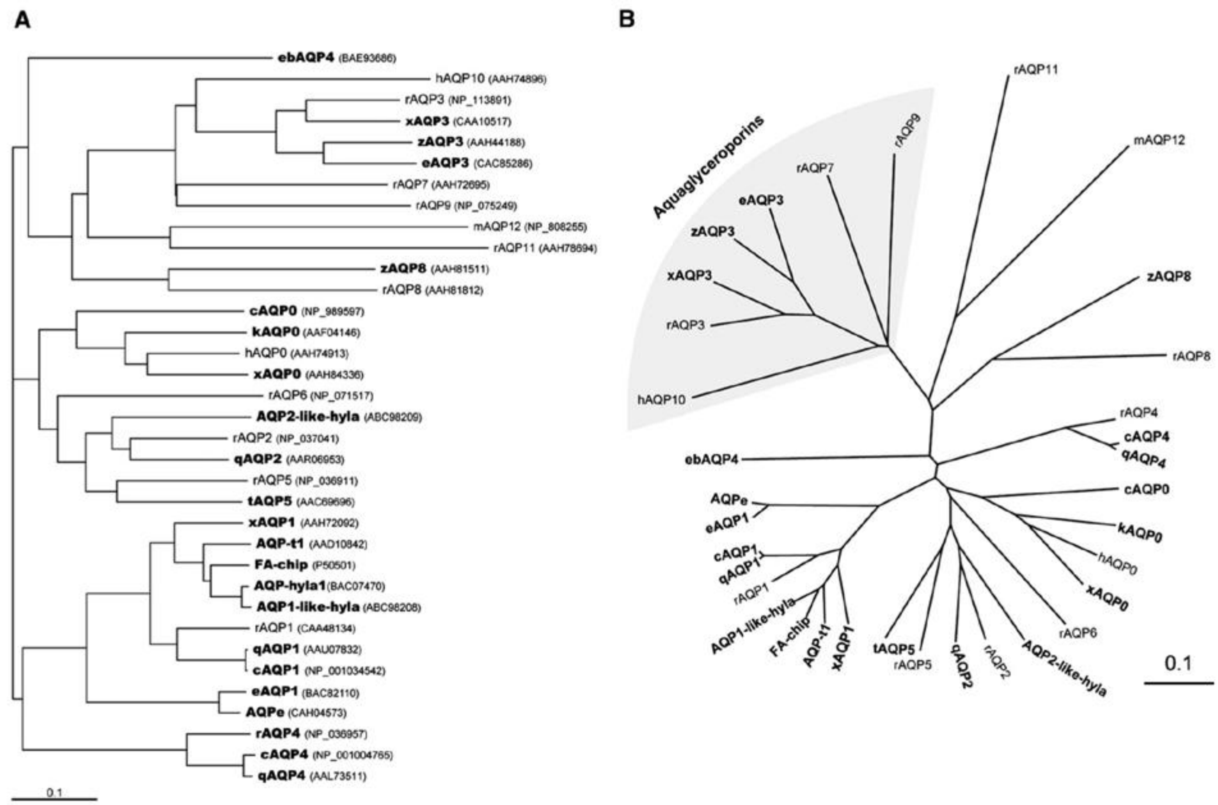

Fig 6.

Amino acid sequences aligned and analyzed by a computerized Clustal X program according to a similarity index. Aquaporins (AQP) and aquaglyceroporins (AQGP) from plants and invertebrates are not included. AQP and AQGP isoform structures reported in GenBank (reference number in parenthesis) were used for analysis. A: The length of the horizontal connecting bars is inversely proportional to the pair-wise similarity scores calculated from the alignment of sequences with use of the Clustal algorithm for PC/GENE. B: Phylogenetic tree of aquaporin superfamily. It suggests a divergence (dichotomy) from the ancestor of the AQP superfamily. AQPs identified in non-mammalian vertebrates are in bold. r: rat; h: human; z: zebrafish; k: killifish; e: eel; x: *X. laevis*; f: frog, t: toad; q: quail; c: chicken; eb*: Eptatretus burgeri* (inshore hagfish); hyla: *Hyla chrysoscelis* (southern gray treefrog).

Table 1

Tissue-specific expression of qAQP4 mRNA by quantitative real-time PCR

	Threshold cycles (C_T)		
Tissues	**18s**	**qAQP4-L/S**	**qAQP4-L**
Lung	13.5±0.2	32.4±0.6	N/A
Heart	13.9±0.4	33.9±1.1	N/A
Liver	13.2±0.4	33.4±0.1	N/A
Muscle	13.5±0.1	31.6±0.1	N/A
Brain	12.8±0.1	20.6±0.0	30.1±0.0
Intestine	14.7±0.1	32.9±0.4	N/A
Adrenal	13.9±0.1	23.4±0.6	33.0±0.7
Medullar	12.9±0.5	27.3±0.1	N/A
Cortex	13.0±0.0	28.3±0.3	N/A